Stopping of swift protons in matter and its implication for astrophysical fusion reactions

C. A. Bertulani[1,2,*] and D. T. de Paula[1,†]
[1]*Instituto de Física, Universidade Federal do Rio de Janeiro, 21945-970 Rio de Janeiro, RJ, Brazil*
[2]*Brookhaven National Laboratory, Physics Department, Upton, New York 11973-5000*
(Received 14 May 2000; published 12 September 2000)

The velocity dependence of the stopping power of swift protons in low-energy collisions is investigated. At low projectile energies the stopping is mainly due to nuclear stopping and charge exchange of the electron. The second mechanism dominates at $E_p \geqslant 200$ eV. A dynamical treatment of the charge exchange mechanism based on two-center electronic wave functions yields transparent results for the exchange probability. We predict that the stopping cross sections vary approximately as $v_p^{1.35}$ for projectile protons on hydrogen targets in the 1 keV energy region.

PACS number(s): 26.20.+f, 34.50.Bw

Nuclear fusion reactions proceed in stars at low energies, e.g., of the order of 10 keV in our Sun [1,2]. At such low energies it is extremely difficult to measure the cross sections for charged-particle-induced fusion reactions at laboratory conditions due to the Coulomb barrier. One often uses a theoretical model to extrapolate the experimental data to the low-energy region. Such extrapolations are sometimes far from reliable, due to unknown features of the low-energy region. For example, there might exist unknown resonances along the extrapolation or even some simple effect which one was not aware of before. One of these effects is the laboratory atomic screening of fusion reactions [3,4]. It is well known that the laboratory measurements of low-energy fusion reactions are strongly influenced by the presence of the atomic electrons. This effect has to be corrected for in order to relate the fusion cross sections measured in the laboratory with those in a stellar environment. Another screening effect, arising from free electrons in the stellar plasma, will not be treated here. For about one decade, until 1996, one observed a large discrepancy between the experimental data and the best models available to treat the screening effect. The simplest (and perhaps the best) of these models, the so-called adiabatic model, predicts that as the projectile nucleus penetrates the electronic cloud of the target the electrons become more bound and the projectile energy increases by energy conservation. Since the fusion cross sections increase strongly with the projectile's energy, this tiny amount of energy gain (of the order of 10–100 eV) leads to a large effect on the measured cross sections. However, in order to explain the experimental data, an extra amount of energy is necessary — about twice the value obtained by the adiabatic model. This is puzzling, since more refined dynamical models, e.g., the time-dependent Hartree-Fock model [5], include electronic excitation and thus yield a screening energy which is smaller than that obtained with the adiabatic model.

This problem was apparently solved in 1996 by Langanke and collaborators [6] and by Bang and collaborators [7], who observed that the experimental data for $^3\mathrm{He}(d,p)^4\mathrm{He}$ — the reaction for which the screening effect was best studied — was probably obtained with an erroneous extrapolation of the stopping power for deuterons in helium targets to the low-energy regime. The fusion reaction occurs at a point inside the target after the projectile has slowed down by interactions with the atomic targets. In the experimental analysis one needs to correct for this energy loss in order to assign the correct projectile energy value for that reaction. These corrections were usually based on the Andersen-Ziegler table of the stopping power of low-energy particles [8]. Because of the lack of experimental information on the stopping power at the extreme low projectile energies needed for astrophysical purposes, the Anderson-Ziegler tabulation was extrapolated to the required energy, another example of a dangerous extrapolation procedure. In fact, Golser and Semrad [9] observed a strong departure of their experimental data from the extrapolations based on the Andersen-Ziegler tables for the stopping of low-energy protons on helium targets. Grande and Schwietz [10] performed a dynamical calculation of the energy dependence of the stopping power for this system and confirmed that the extrapolation procedure cannot be extended to very low energies. Whereas at higher energies the stopping is mainly due to the ionization of the target electrons, at astrophysical energies it is mainly due to charge exchange between the target and the projectile. References [6] and [7] used these arguments to explain the long-standing discrepancy between theory and experiment for the low-energy dependence of the reaction $^3\mathrm{He}(d,p)^4\mathrm{He}$. Other reactions of astrophysical interest (e.g., those listed in by Rolfs and co-workers [3,4]) should also be corrected for this effect.

In this work we address the problem of the stopping of very-low-energy ions in matter. To simplify matters, we study the simplest system $p+\mathrm{H}$. It displays important features of the stopping power and has the advantage of allowing a simple solution.

Our approach is based on the solution of the time-dependent Schrödinger equation for the electron in a dynamical two-center field. The static two-center $p+\mathrm{H}$ system was solved by Teller in 1930 [11]. He showed that as the distance between the protons decreases the hydrogen orbitals split into two or more orbitals, depending on its degeneracy in the two-center system. Analogous problems are well known in quantum systems [12]. For example, take two identical potential wells at a certain distance. For large distances

*Electronic address: bertu@if.ufrj.br
†Electronic address dani@if.ufrj.br

the states in one well are degenerated with regard to the states in the other potential well. As they approach this degeneracy is removed due to the influence of barrier tunneling. Thus, the lowest-energy state of hydrogen, $1s$, splits into the $1s\sigma$ and the $2p\sigma$ states as the protons approach each other. The $1s\sigma$ state is space symmetrical, while the $2p\sigma$ state is antisymmetric. As the proton separation distance decreases their respective energies decrease. At $R\simeq 1$ Å the energy of the $2p\sigma$ state starts to increase again, while the energy of the $1s\sigma$ state continues to decrease. For proton distances much smaller than 1 Å the $1s\sigma$ and the $2p\sigma$ energies correspond to those of the first and second states of the He atom, respectively [11].

Let us now consider the dynamical case. The full time-dependent wave function for the system can be expanded in terms of two-center states $\phi_n(t)$ governed by the Schrödinger equation

$$[H_0+V_p(t)]\phi_n(t)=E_n(t)\phi_n(t),$$

$$\text{with}\quad H_0=\hat{\mathbf{p}}_e^2/2m_e+V_T, \tag{1}$$

where $V_p(t)=-e^2/|\mathbf{r}+\mathbf{R}/2|$ is the electron-projectile proton interaction potential and $V_T=-e^2/|\mathbf{r}-\mathbf{R}/2|$ is the electron-target proton interaction for a proton-proton separation distance $R(t)$. Note that in our formulation the two-center wave functions depend on time, as well as their energies $E_n(t)$. The full electronic wave function is obtained by a sum over all orthonormal two-center states:

$$|\Psi(t)\rangle=\sum_n a_n(t)|\phi_n(t)\rangle,$$

$$\text{with}\quad \int d^3r\,\phi_n(t)\phi_m(t)=\delta_{nm}. \tag{2}$$

Inserting this expansion into Eq. (1) we obtain

$$i\hbar\frac{d}{dt}a_m(t)=E_m(t)a_m(t)-i\hbar\sum_n a_n(t)\left\langle m\left|\frac{d}{dt}\right|n\right\rangle. \tag{3}$$

Using Eq. (1) one can easily show that, for $m\neq n$,

$$\left\langle m\left|\frac{d}{dt}\right|n\right\rangle=\frac{\langle m|dV_p/dt|n\rangle}{E_n(t)-E_m(t)},\quad (m\neq n). \tag{4}$$

Moreover, using the second relation of Eq. (2), one can show that $\langle m|d/dt|m\rangle=0$, if $|m\rangle$ is real. This indeed will be our case. Our basis $|n(t)\rangle$ is formed by two-center states at a given time t, i.e., a given proton separation distance $R(t)$. These wave functions are real. Thus, the final coupled-channels equation for the two-center problem is given by

$$i\hbar\frac{d}{dt}a_m(t)=E_m(t)a_m(t)-i\hbar\sum_{m\neq n}a_n(t)\frac{\langle m|dV_p/dt|n\rangle}{E_n(t)-E_m(t)}. \tag{5}$$

At very low proton energies ($E_p\lesssim 1$ keV) it is fair to assume that only the low-lying states are involved in the electronic dynamics. Only at proton energies of the order of 25 keV is the proton velocity comparable to the electron velocity $v_e\simeq\alpha c$. Thus, the evolution of the system is almost adiabatic at $E_p\lesssim 10$ keV. The higher states require too much excitation energy and belong to different degeneracy multiplets. The initial electronic wave function is a superposition of $1s\sigma$ and $2p\sigma$ two-center states. One thus expects that only these states are relevant for the calculation. In fact, at these energies the population of the $2p$ atomic state in charge exchange is much less than the population of the $1s$ atomic state. These assumptions are well supported by the calculations of Grande and Schwietz [10], who have used a dynamical approach based on target-centered wave functions. In their approach one has to include a great amount of target-centered states in order to represent well the strong distortion of the wave function as the projectile closes in the target. We also have assumed that the proton follows a classical trajectory determined by an impact parameter b.

Equation (5) does not look like the usual form of coupled-channels equations in the theory of the time-dependent Schrödinger equation. But we can put it in such form by rewriting the equation as

$$i\hbar\frac{d}{dt}\begin{pmatrix}a_+\\ a_-\end{pmatrix}=\begin{pmatrix}V_++E_0 & iW\\ iW & V_-+E_0\end{pmatrix}\begin{pmatrix}a_+\\ a_-\end{pmatrix}, \tag{6}$$

where the indices $+$ and $-$ refer to the $1s\sigma$ and $2p\sigma$ states, respectively, $E_0=-13.6$ eV, $V_\pm(t)=E_\pm(t)-E_0$, and

$$W(t)=\hbar\frac{\langle\Psi_+|dV_p/dt|\Psi_-\rangle}{E_+(t)-E_-(t)}\equiv\hbar\frac{\langle\Psi_{1s\sigma}(t)|dV_p/dt|\Psi_{2p\sigma}(t)\rangle}{E_{1s\sigma}(t)-E_{2p\sigma}(t)}. \tag{7}$$

In this form, the potentials $V_\pm(t)$ and $W(t)$ act like potentials in the usual coupled-channels equations. We use the formalism of Teller [11] to calculate the wave functions $\Psi_\pm(R)$ at different interproton distances $R(t)$ corresponding to a particular time t. The static Schrödinger equation is solved in elliptical coordinates. This yields two coupled differential equations which can be solved by expanding the solutions in a Taylor series. A set of recurrence relations is obtained for the expansion coefficients when the boundary conditions are used. The energies $E_{1s\sigma}(R)$ and $E_{2p\sigma}(R)$ are obtained by adjusting the constant which separates the two coupled equations [11] to its correct matching value.

When $t\to\pm\infty$, $V_\pm\to 0$ and $W\to 0$. The initial state, an electron localized in the target, can be written in terms of the degenerate symmetric, $\Psi_+=\Psi_{1s\sigma}$, and antisymmetric, $\Psi_-=\Psi_{2p\sigma}$, states:

$$\Phi_T=\frac{1}{\sqrt{2}}(\Psi_++\Psi_-),\quad \text{at}\ \ t\to-\infty, \tag{8}$$

where both Φ_T and $\Psi_\pm$ are normalized wave functions. If the electron is localized in the projectile, the wave function $\Phi_p=(\Psi_+-\Psi_-)/\sqrt{2}$, when $t\to-\infty$, is used. We will consider only the condition of Eq. (8), namely, an electron localized at the target at $t\to-\infty$. These relations are well-

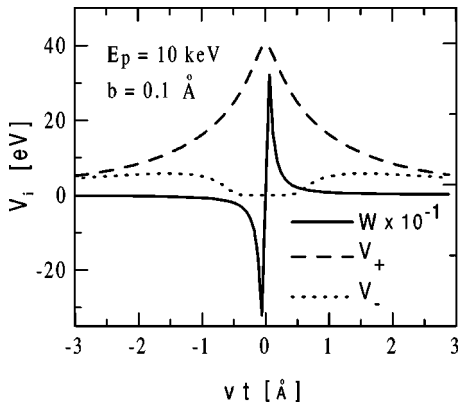

FIG. 1. Time dependence of the interaction potentials $V_{\pm}(t)$ and $W(t)$ for $E_p=10$ keV and a nearly central collision $b=0.1$ Å .

known quantum mechanical results; the asymptotic two-center wave functions can be written as combinations of target- and projectile-centered $1s$ wave functions: $\Psi_{\pm}=(\Phi_p \pm \Phi_T)/\sqrt{2}$.

Starting with a target localized electron we assign the initial conditions $a_{\pm}=1/\sqrt{2}$ at $t\rightarrow-\infty$ and solve Eq. (6) numerically. Although at $t\rightarrow+\infty$ the probabilities $|a_{\pm}|^2$ remain very close to 1/2, the amplitudes $a_{\pm}$ acquire phases which change the relative population of the projectile and the target 1s state. We correct for energy conservation which feeds the increasing binding energy of the electron back to an increasing relative motion energy of the two protons as they come closer. This is specially important as E_p becomes of the order of hundreds of eV and smaller. In Fig. 1 we show the time dependence of $V_{\pm}(t)$ and $W(t)$ for $E_p=10$ keV and a nearly central collision, $b=0.1$ Å . One observes that the potentials $V_{\pm}(t)$ extend much farther out than $W(t)$. Moreover, we find that as E_p decreases the potential W decreases faster than the projectile's velocity v_p. This is mainly due to the derivative of V_p in Eq. (7). At $E_p\simeq 100$ eV the potential W loses its relevance as compared to $V_{\pm}$, which have no dependence on v_p. This becomes clear in Fig. 2. In this figure we show the exchange probability as a function of the impact parameter for two projectile energies. The solid line is the full solution of Eq. (6). The dashed line is the approximation obtained when we set $W=0$ in Eq. (6). In the latter case, the equations decouple and it is straightforward to show that the exchange probability is given by

$$P_{exch}=\Big|\sum_{\pm} a_{\pm}(\infty)\langle\Phi_T|\Psi_{\pm}(\infty)\rangle\Big|^2$$

$$=\frac{1}{2}+\frac{1}{2}\cos\left\{\frac{1}{\hbar}\int_{-\infty}^{\infty}[E_-(t)-E_+(t)]dt\right\}. \qquad (9)$$

At $E_p=10$ keV there is an appreciable difference between the full calculation and the approximation (9). But for $E_p=100$ eV the results are practically equal, except for very small impact parameters at which the potential W still has an effect.

One observes that the exchange probability is not constant at small impact parameters, but oscillates wildly around 0.5,

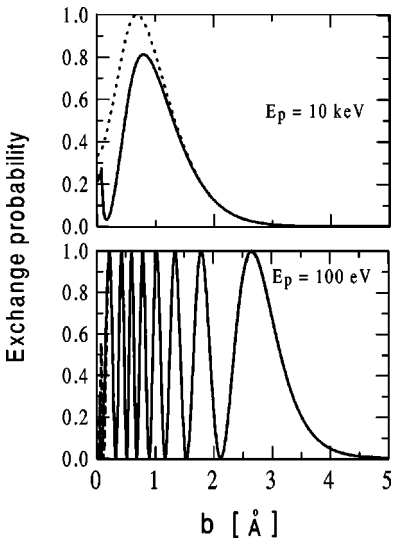

FIG. 2. The exchange probability as a function of the impact parameter for two projectile energies. The solid line is the full solution of Eq. (6). The dashed line is the approximation obtained when we set $W=0$ in Eq. (6).

especially for low projectile energies. One might naively assume that because the collision is almost adiabatic, the system loses memory of to which nucleus the electron is bound after the collision. Thus, for small impact parameters one would expect a 50% probability of finding the electron in one of the nuclei at $t=\infty$. However, this is not what happens. From Eq. (9) we see that minima of the probability occur for impact parameters satisfying the relation

$$\int_{-\infty}^{\infty}[E_-(t)-E_+(t)]dt=2\pi\hbar(n+1/2), \quad n=0,1,2,\ldots,N. \qquad (10)$$

This relation looks familiar, of course. It simply states that the interference between the $1s\sigma$ and the $2p\sigma$ states induces oscillations in the exchange probability. The electron tunnels back and forth between the projectile and the target during the ingoing and the outgoing parts of the trajectory. When the interaction time is an exact multiple of the oscillation time, a minimum in the exchange probability occurs. The average probability over the smaller impact parameters is indeed 0.5. As the impact parameter decreases from infinity, the first maximum in the exchange probability indicates the beginning of the region of strong exchange probability. One sees that at low proton energies this starts at $b\simeq 3$ Å . The size of the hydrogen atom is about 0.5 Å and thus the electron travels in a forbidden region (tunnels) of about 2 Å from the target to the projectile. This is possible because of the strong interference between the $1s\sigma$ and the $2p\sigma$ states, which for some trajectories satisfy the quantum relation (10).

To obtain the stopping power we need the total cross section for charge exchange, $\sigma=2\pi\int P_{exch}bdb$. This is shown in Fig. 3. The solid line is the full coupled-channels calculation, while the dashed line uses approximation (9) for the exchange probability. We observe that the approximation (9) reproduces well the full calculation even at the highest ener-

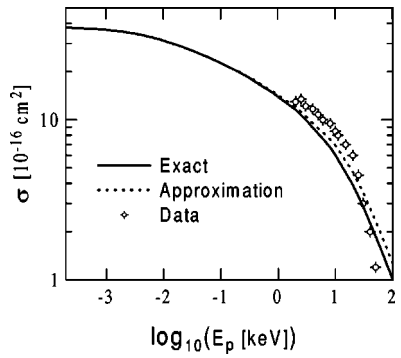

FIG. 3. The solid line is the full coupled-channels calculation for the charge-exchange cross section, while the dashed line uses approximation (9) for the exchange probability. The experimental data are from McClure [13].

gies. The reason is that the potential W is always smaller than $V_{\pm}$ for large impact parameters which have more weight on the integral cross section. We also compare our calculations with the lowest energy data of McClure [13]. The formalism developed here is inappropriate for energies in the tens of keV range and higher, as the projectile velocity becomes comparable to or higher than the electron velocity. This implies that two-center states with higher energy and even continuum states (ionization) should be included in the calculation. For $E_p \rightarrow 0$, the charge exchange cross section becomes the constant value $\sigma(E_p=0)=37.88\times10^{-16}$ cm^2. This happens because, when $E_p \rightarrow 0$ and as the projectile nears the target, the increasing electron binding in the two-center system acts as a push in the relative motion energy to compensate for energy conservation. The average result is that the cross section for charge exchange becomes approximately constant for projectile energies of tens of eV and below.

In Fig. 4 we show the stopping cross section of the proton. The stopping cross section is defined as $S=\Sigma_i \Delta E_i \ \sigma_i$, where ΔE_i is the energy loss of the projectile in a process denoted by i. The stopping power $S_P=dE/dx$, the energy loss per unit length of the target material, is related to the stopping cross section by $S=S_P/N$, where N is the atomic density of the material. In our charge-exchange mechanism the electron is transferred to the ground state of the projectile and the energy transfer is given by $\Delta E = m_e v_p^2/2$, where v_p is the projectile velocity. Assuming that there are few free electrons in the material (e.g., in a hydrogen gas) only one more stopping mechanism at very low energies should be considered: the nuclear stopping power. This is simply the elastic scattering of the projectile off the target nuclei. The projectile energy is partially transferred to the recoil energy of the target atom. The stopping cross section for this mechanism has been extensively studied by Lindhard and collaborators (e.g., Ref. [14]). The nuclear stopping includes the effect of the electron screening of the nuclear charges.

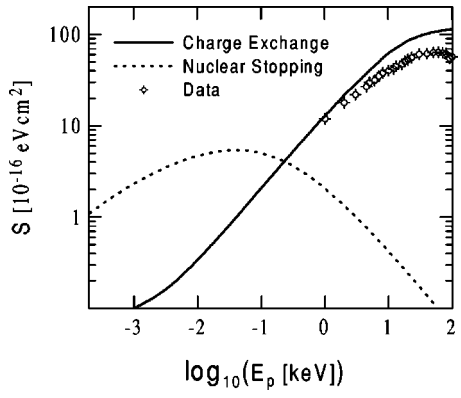

FIG. 4. The stopping cross section of protons on H targets. The dotted line gives the energy transfer by means of nuclear stopping, while the solid line is our result for the charge-exchange stopping mechanism. The data points are from the tabulation of Andersen and Ziegler [8].

The dotted line in Fig. 4 gives the energy transfer by means of nuclear stopping, while the solid line are our results for the charge-exchange stopping mechanism. The data points are from the tabulation of Andersen and Ziegler [8]. We see that the nuclear stopping dominates at the lowest energies, while the charge-exchange stopping is larger for proton energies greater than 200 eV. Since we neglect the difference between molecular and atomic hydrogen targets, there is a limitation to compare our results with the experimental data. But the order of magnitude agreement is good in view of our simplifying assumptions. We do not consider the change of the charge state of the protons as they penetrate the target material. The exchange mechanism transforms the protons into H atoms. These again interact with the target atoms. They can lose their electron again by transfer to the $1s$ state of the target [10].

The best fit to our calculation for the stopping power for proton energies in the range 100 eV to 1 keV yields $S \sim v_p^{1.35}$. This contrasts with the extrapolation $S \sim v_p$, based on the Andersen-Ziegler table. But this discrepancy is much less than the one obtained by Golser and Semrad [9] for helium targets, who found a stopping power for protons $S \sim v_p^{3.34}$ for protons in the energy range of 4 keV. No data at lower energies are available in this case. But the Golser and Semrad data, for proton energies above 3 keV, firmly indicate that a high power dependence on the projectile velocity will be also valid at lower energies, in contrast to the predictions from the Andersen-Ziegler tables [8]. One cannot extend our calculations to helium targets as the initial wave function cannot be described in terms of a simple sum of two-center states. A much larger two-center basis is necessary. Since the electrons in the helium target are more bound than in the proton, the charge-exchange probability must be much smaller than in the case of hydrogen targets. One thus should indeed expect a much stronger dependence of the stopping on the projectile velocity. At very low energies, of the order of some hundreds of eV, the stopping cross section should be entirely dominated by nuclear stopping, even more than for hydrogen targets.

The $p+p \rightarrow d+e^+ +\nu_e$ reaction is a very important one occurring in, e.g., our Sun. But it proceeds via the weak interaction and its cross section is too small for studies under the laboratory conditions [1,2]. Fortunately, a good theoreti-

cal model exists for this reaction [16]. Other reactions could be strongly influenced by the stopping power of protons and deuterons due to the charge-exchange mechanism. They can be relevant for the study of $d+\mathrm{D}$ reactions in stellar interiors and fusion reactors. Another application is the $\mathrm{D}(p,\gamma)^3\mathrm{He}$ reaction which is important for the hydrogen burning in stars. In our Sun the most effective energy of this reaction is $E_{\mathrm{c.m.}}=6.5\pm3.3$ keV at $T=15\times10^6$ K. At this energy one expects that the charge-exchange stopping cross section should be as important as the ionization cross section. Experimental data exist at the lowest energy value of 16 keV [15,17]. Although the extrapolation based on theory appears to be under control in this case, it is worthwhile to consider a better study of the stopping power for this reaction. The steep rise of the fusion cross sections at astrophysical energies amplifies all effects leading to a slight modification of the projectile energy [18]. Our results show that the stopping mechanism does not follow a universal pattern for all systems. This calls for improved theoretical studies of charge-exchange effects and for their independent experimental verification.

We would like to express our gratitude to Prof. A.B. Balantekin, Prof. S.R. Souza, and Prof. L.F. Canto for useful comments and suggestions during the development of this work. This work was partially supported by the Brazilian agencies CNPq, FAPERJ, FUJB, and by the MCT/ FINEP/ CNPq(PRONEX) (Contract No. 41.96.0886.00). C.A.B. acknowledges the support of the John Simon Guggenheim Memorial Foundation.

[1] D.D. Clayton, *Principles of Stellar Evolution and Nucleosynthesis* (McGraw-Hill, New York, 1968).
[2] C. Rolfs and W.S. Rodney, *Cauldrons in the Cosmos* (Chicago Univeristy Press, Chicago, 1988).
[3] H.J. Assenbaum, K. Langanke, and C. Rolfs, Z. Phys. A **327**, 461 (1987).
[4] E. Somorjai and C. Rolfs, Nucl. Instrum. Methods Phys. Res. B **99**, 297 (1995).
[5] T.D. Shoppa, S.E. Koonin, K. Langanke, and R. Seki, Phys. Rev. C **48**, 837 (1993).
[6] K. Langanke, T.D. Shoppa, C.A. Barnes, and C. Rolfs, Phys. Lett. B **369**, 211 (1996).
[7] J.M. Bang, L.S. Ferreira, E. Maglione, and J.M. Hansteen, Phys. Rev. C **53**, R18 (1996).
[8] H. Andersen and J.F. Ziegler, *The Stopping and Ranges of Ions in Matter* (Pergamon, New York, 1977), Vol. 3.
[9] R. Golser and D. Semrad, Phys. Rev. Lett. **14**, 1831 (1991).
[10] P.L. Grande and G. Schiwietz, Phys. Rev. A **47**, 1119 (1993); **58**, 3796 (1998); Nucl. Instrum. Methods Phys. Res. B **153**, 1 (1999).
[11] E. Teller, Z. Phys. **61**, 458 (1930).
[12] E. Merzbacher, *Quantum Mechanics* (Wiley, New York, 1997).
[13] G.W. McClure, Phys. Rev. **148**, 47 (1966).
[14] J. Lindhard, M. Scharff, and H.E. Shiøtt, Mat. Fys. Medd. K. Dan. Vidensk. Selsk. **33**, 1 (1963).
[15] G.M. Griffiths, M. Lal, and C.D. Scharfe, Can. J. Phys. **41**, 724 (1963).
[16] J.N. Bahcall, *Neutrino Astrophysics* (Cambridge University Press, Cambridge, 1989).
[17] G.M. Bailey, G.M. Griffiths, M.A. Olivo, and R.L. Helms, Can. J. Phys. **48**, 3059 (1970).
[18] A.B. Balantekin, C.A. Bertulani, and M.S. Hussein, Nucl. Phys. **A627**, 324 (1997).